

Communication

200 Gbps/λ PON Downstream C-Band Direct-Detection Links with ≥ 29 dB Power Budget

Haoyi Wang ¹ , Pablo Torres-Ferrera ¹, Giuseppe Rizzelli ^{1,2,*}, Roberto Mercinelli ³, Valter Ferrero ¹ and Roberto Gaudino ¹

¹ Department of Electronics and Telecommunications, Politecnico di Torino, Corso Duca degli Abruzzi 24, 10129 Torino, Italy; haoyi.wang@polito.it (H.W.); pablo.torres@polito.it (P.T.-F.); valter.ferrero@polito.it (V.F.); roberto.gaudino@polito.it (R.G.)

² LINKS Foundation, Via Pier Carlo Boggio 61, 10138 Torino, Italy

³ Technology Innovation Cloud Access Solutions, Telecom Italia (TIM), Via Reiss Romoli 274, 10148 Torino, Italy; roberto.mercinelli@telecomitalia.it

* Correspondence: giuseppe.rizzelli@linksfoundation.com

Abstract: In this paper we present the simulative analysis of a 200 Gbps per wavelength (λ) 8-level pulse amplitude modulation (PAM-8) downstream communication over up to 20 km single mode fiber (SMF) in C-band based on direct detection (DD) achieving at least a 29 dB link power budget in a PON environment. We use chromatic dispersion digital pre-compensation (CD-DPC) and a dual-arm in-phase and quadrature Mach-Zehnder modulator (IQ-MZM) at the optical line termination (OLT) side, while preserving DD in the optical network unit (ONU). Three receiver digital-signal-processing (DSP) options are analyzed and compared: square-root-like technique (SQRT) in combination with a feed forward equalizer (FFE) and a decision feedback equalizer (DFE), the Volterra nonlinear equalizer (VNLE), and the SQRT in combination with the VNLE. The SQRT can be applied in combination with the VNLE to decrease the receiver DSP complexity while maintaining the required system performance. We show that PAM-8 with CD-DPC and the SQRT in combination with the VNLE is a feasible solution for 200 Gbps per λ downstream C-band transmission for PON.



Citation: Wang, H.; Torres-Ferrera, P.; Rizzelli, G.; Mercinelli, R.; Ferrero, V.; Gaudino, R. 200 Gbps/λ PON Downstream C-Band Direct-Detection Links with ≥ 29 dB Power Budget. *Appl. Sci.* **2022**, *12*, 3538. <https://doi.org/10.3390/app12073538>

Academic Editor: John Xiupu Zhang

Received: 25 February 2022

Accepted: 29 March 2022

Published: 30 March 2022

Publisher's Note: MDPI stays neutral with regard to jurisdictional claims in published maps and institutional affiliations.



Copyright: © 2022 by the authors. Licensee MDPI, Basel, Switzerland. This article is an open access article distributed under the terms and conditions of the Creative Commons Attribution (CC BY) license (<https://creativecommons.org/licenses/by/4.0/>).

1. Introduction

Next-generation passive optical networks (PON) have been under rapid development to fulfill the ever-increasing bandwidth and traffic requirements in the access and short-reach communications segment. The standardization of higher speed PON targeting 50 Gbps per wavelength (λ) has been recently performed by ITU-T [1–4]. However, next-generation 5G and 6G systems will require even higher data rates, and PONs represent a suitable practical technology to support future optical access solutions [5–8]. Currently, research efforts are targeting data rates of 100 Gbps per λ and beyond [9–17] for the next step of PON evolution.

The latest PON standards (i.e., 25G-PON and 50G-PON) have chosen the direct detection (DD) scheme to meet cost requirements, and O-band operations for both upstream (US) and downstream (DS) directions to cope with chromatic dispersion [1–4]. However, the penalty due to chromatic dispersion is not negligible at high data rates, such as 200 Gbps, even in the O-band. Compared to the O-band, the C-band can provide a lower optical loss and optical nonlinearity. For higher speed PON upgrades, backward compatibility with legacy Gigabit PON (G-PON) (currently, one of the most commonly deployed PON standards) can be achieved in the C-band by reusing the 1480–1550 nm wavelength range of the downstream. Moreover, the O-band window might become filled, opening to the possibility of considering the C-band again in future PON standardization efforts. To achieve this, dispersion must be compensated. Coherent detection is well-known to allow

compensation of CD, power-fading effect and other impairments through digital signal processing, thus enabling C-band operation. In [18–20], the possibility of using coherent detection has been studied. However, due to the high cost and complexity, the use of coherent detection in the cost-effective PON environment is still under discussion [9,18]. In a recent work [15], we proposed chromatic dispersion digital pre-compensation (CD-DPC) for 100 Gbps links using a dual-arm in-phase and quadrature Mach–Zehnder modulator (IQ-MZM) at the transmitter (TX) side while keeping DD at the receiver (RX). This approach only increases complexity at the optical line termination (OLT) side, which in the PON downstream scenario is shared among the end users.

Increasing the target data rate requires pushing the system into nonlinear operation [16,17,21] to be able to increase the transmitter launch power and the optical modulation index to achieve the demanding power–budget requirements. In [16], we analyzed simple nonlinear compensation techniques, i.e., square-rootlike (SQRT) and polynomial (POLY) techniques. We simulatively and experimentally confirmed about 2 dB gain in terms of maximum optical distribution network (ODN) loss for a 100 Gbps downstream transmission, thanks to SQRT and POLY.

Next generation PONs must be backward compatible with legacy PONs, and the ODN must remain the same. Typically, at least a 29 dB link power budget (budget class N1) and a 0 to (at least) 20 km fiber reach must be guaranteed [1–4,22]. Regarding the trend of ITU-T PON standardization evolution, at least a 4-fold increment in DS capacity can be observed between 2 consecutive PON system generations [2,4]. For example, there is a 4-fold increment in DS capacity from a GPON (with DS 2.5 Gbps per λ) to XG(S)-PON (with DS 10 Gbps per λ), and a 5-fold increment from a XG(S)-PON to a higher speed PON (with DS 50 Gbps per λ). Therefore, it is expected that the next generation beyond 50G-PON will target (at least) 200 Gbps per λ in DS. To meet the 29 dB ODN loss and 20 km fiber reach at 100 Gbps is very challenging, as we showed in previous works [14–17]. For a 200 Gbps per λ transmission, the situation becomes extremely critical. In this paper, we focus on 200 Gbps per λ transmission in a C-band to guarantee 29 dB ODN loss over a 20 km fiber link, by combining the CD-DPC algorithm with two nonlinear distortion compensation techniques: the SQRT [16] and the Volterra nonlinear equalizer (VNLE) [17]. In [17], for 100 Gbps per λ transmission in a C-band, we experimentally showed a 1–2 dB gain in term of ODN loss by using VNLE when compared to the SQRT.

Until now, non-return-to-zero on-off-keying (NRZ-OOK) modulation format has been defined for all standardized PONs. It is expected that 50G class optoelectronics (O/E) will be commercially available by the time 200 Gbps products are developed. However, devices to support OOK and 4-level pulse amplitude modulation (PAM-4) operations at 100 Gbaud or beyond seems difficult to achieve in the midterm [3,23]. Thus, we consider 8-level PAM (PAM-8) as a candidate modulation format for 200 Gbps transmission to have a reduced baud rate (i.e., around 66.67 Gbaud for 200 Gbps bit rate). In [13], a 200 Gbps PAM-4 communication with a 29 dB ODN loss was experimentally demonstrated by using directly modulated laser (DML), direct detection and Raman amplification over a 21 km fiber. However, very high transmitter and receiver bandwidth devices, i.e., a 65 GHz DML and 70 GHz P-type-intrinsic-N-type diodes (PIN), were used in the experiments. Moreover, the strong Raman pumping used in the experiments is not suited for a cost-effective short-reach PON. In this paper, we demonstrate over 29 dB of ODN loss using 50G O/E devices without Raman amplification. In a 50G PON, the maximum launched power into ODN is +7, +9, +11 and +11 dBm for budget class N1, N2, E1 and E2, respectively [24]. For 50G PON with a higher budget class, for example Class C+ (32 dB) and beyond, a minimum launched power of +10 dBm might be required. In PONs, a launch power a few dB higher than the minimum one can be tolerated [25]. Transmitted optical power (TOP) could be increased to achieve the required link power budget. An electro absorption modulated laser (EML) boosted by an external semiconductor optical amplifier (SOA) can be placed at the TX side to increase launch power in PONs for a wide wavelength range of 1200–1650 nm [26]. For a 50G PON, EML + SOA was exploited DS to support high budget classes. In [25], a 14 dBm

launch power was emulated by using EML + SOA. In [27], an integrated EML + SOA with a 13 dBm output power was experimentally demonstrated to achieve a 35 dB link budget. In our previous works for 100 Gbps transmission, we used a TOP of 11 dBm. In this paper, we increase it to 15 dBm (when the VNLE is applied) to achieve the 29 dB power–budget requirements for 200 Gbps transmission.

The paper is organized as follows: the details of the simulation setup and simulated parameters are described in Section 2. In Section 3, we analyze the proposed system performance through simulations with variable transceiver bandwidth and for different RX DSP options. The complexity of different RX DSP options is compared in terms of multiplication per sample (MPS). Lastly, we discuss the results and draw some conclusions in Section 4.

2. Simulation Setup

The simulation setup is schematically illustrated in Figure 1. Single channel transmission is considered. At the TX side, a PRBS-15 pseudorandom binary sequence is generated at bit rate $R_b = 200$ Gbps, and then coded to generate a PAM-8 sequence. As shown in Figure 1, the CD-DPC algorithm is implemented based on a finite impulse response (FIR) complex filter, which is explained in detail in [15]. The key idea behind this algorithm is the following: the fiber length L is known in advance and the accumulated CD is $D \cdot L$ ps/nm (where D is the dispersion coefficient). An electrical transmitted signal is sent to the FIR filter-based CD-DPC block, which works at m samples per symbol (SpS) with N_t taps. The CD-DPC block is placed at the TX side digital signal processing (DSP) and emulates the inverse of the CD accumulated along the link. A proper value of pre-compensated length L_C must be set in the CD-DPC block to design the taps of the FIR filter. As a result, an accumulated CD of $D \cdot L_C$ ps/nm is assumed to be pre-compensated. There could be a mismatch ΔL between L and L_C , ($\Delta L = L_C - L$), which the system should tolerate. In [14–17], we demonstrated a tolerance on ΔL of about ± 2 km in a C-band for a 100 Gbps transmission through simulations and experiments. In this paper, the CD-DPC DD works at $m = 2$ SpS and $N_t = 80$. The I and Q arm of the dual-arm IQ-MZM are driven by two real-valued in-phase $I(n)$ and quadrature $Q(n)$ signals biased at quadrature and null point, respectively. The peak-to-peak amplitude V_{PP} of signal $I(n)$ and $Q(n)$, i.e., $V_{PP,I}$ and $V_{PP,Q}$ respectively, are measured at the input of the IQ-MZM. $V_{PP,I}$ and $V_{PP,Q}$ must be optimized to obtain the best system performance by optimizing a scaling factor (the parameter k in Figure 1, which is the same for both $I(n)$ and $Q(n)$ signal). The simulator is explained in detail in [15]. The bias voltage of the IQ-MZM V_π is 5 V.

The modulated optical signal in C-band at wavelength $\lambda = 1550$ nm is propagated over a conventional ITU-T G.652 single mode fiber (SMF) with length $L = 20$ km (typical for PON). The fiber attenuation, chromatic dispersion D and non- linear coefficient n_2 are set to 0.22 dB/km, 17 ps/(nm·km) and 26×10^{-21} m²/W, respectively. The effective area is $80 \mu\text{m}^2$ [28]. Kerr nonlinearities are introduced using the conventional nonlinear Schrödinger equation (NLSE) solved numerically by the split-step Fourier method. The received optical power (ROP) is measured after a variable optical attenuator (VOA) is used to emulate the ODN loss. Second order low-pass super Gaussian filters (SGF) are used to emulate the O/E bandwidth limitations with the same -3 dB bandwidth f_{3dB} both at TX and RX side. We analyze the impact of transceiver bandwidth limitations varying f_{3dB} from 30% to more than 100% of the baud rate, i.e., from 20 GHz to 70 GHz. At the RX side, an optical filter with a 75 GHz bandwidth is placed between the SOA and PIN. The receiver simulated parameters are SOA gain $G = 11$ dB, SOA noise figure $NF = 7$ dB, photodiode responsivity $R = 0.7$ A/W, and transimpedance amplifier (TIA) input referred noise density $IRND = 12$ pA/sqrt(Hz). A digital-to-analog converter (DAC) and an analog-to-digital converter (ADC) with a 6 bits resolution for quantization are used to emulate the arbitrary waveform generator (AWG) and real-time oscilloscope (RTO), respectively.

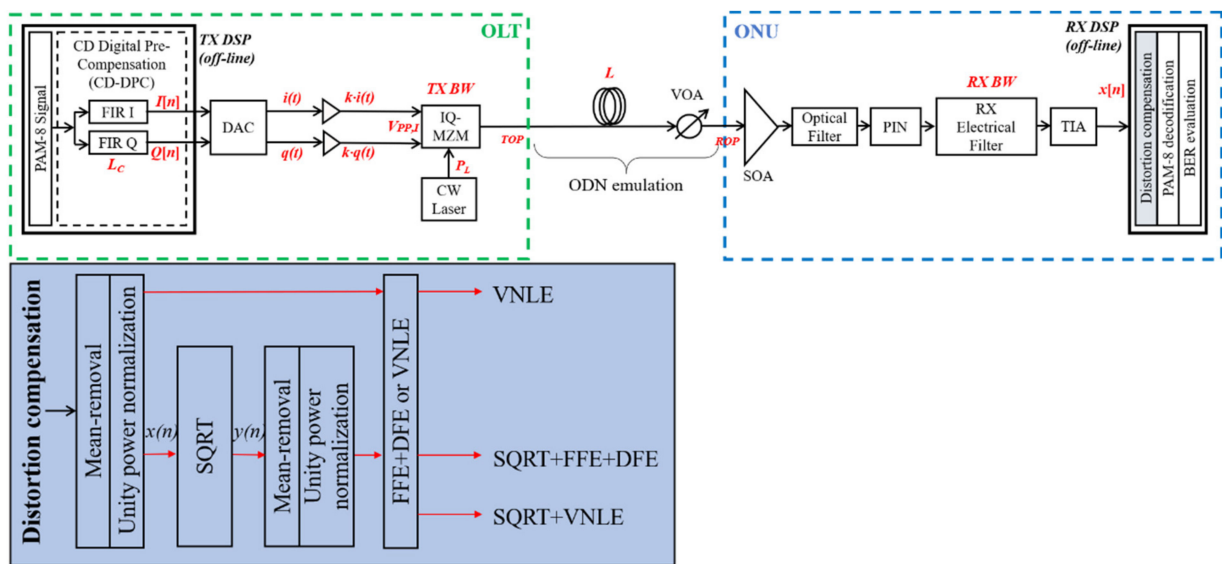


Figure 1. Simulation setup of the proposed CD-DPC DD link, emulating a PON downstream transmission. Dispersion compensation blocks with different DSP options are indicated.

In the off-line DSP at the receiver, the digitized sequence is down sampled and off-line processed at 2 SpS, using one of the three DSP nonlinear distortion compensation methods shown at the bottom of Figure 1. As detailed in [16], the SQRT exploits a square-rootlike function, i.e., $y(n) = \sqrt{x(n) + \min(x(n))}$, and POLY consists of a polynomial function, i.e., $y(n) = x(n) + \alpha x^2(n)$, where $x(n)$ and $y(n)$ are the input and output signal of the SQRT (or POLY) block as shown in Figure 1, and α is a free parameter to be optimized. Since we also showed that a SQRT can provide a similar gain as POLY, but with lower complexity, in this paper we will consider the SQRT. We also analyze a technique based on the VNLE. To keep the complexity low, the VNLE is limited to third order, i.e., linear, quadratic, and cubic terms are considered [29]. In our simulations, we set quadratic memory and cubic memory to be the same, and term them as nonlinear memory (NL memory). For example, *NL memory* = 5 samples means *quadratic memory* = *cubic memory* = 5 samples. The three DSP nonlinear distortion compensation methods are: (i) the SQRT [16,30] in combination with a 120-taps feed forward equalizer (FFE) and a 5 taps decision feedback equalizer (DFE). We indicate it as “SQRT + FFE + DFE”. (ii) VNLE with 121 linear memory and a variable number of NL memory, ranging from 5 samples to 20 samples. We indicate it as “VNLE”. (iii) The SQRT in combination with the same VNLE as in option (ii). We indicate it as “SQRT + VNLE”. The SQRT + FFE + DFE method is equivalent to the VNLE method with *NL memory* = 0. The transmitted optical power *TOP* is set to 15 dBm for options with the VNLE (i.e., VNLE and SQRT + VNLE) and 11 dBm for the option without the VNLE (i.e., SQRT + FFE + DFE).

The typical metric used in a PON performance evaluation is the achievable ODN loss, calculated as the ratio between the TOP and the ROP. In this manuscript, we consider the required ROP (RROP) to obtain a BER target $BER_T = 10^{-2}$ (low-density parity check (LDPC) code forward error correction (FEC) scheme), and we will show system performance in terms of the maximum ODN loss that that guarantees operation equal to or below the BER_T (*Maximum ODN loss [dB] = TOP [dBm] – RROP [dBm]*).

3. Simulation Results

In our simulation setup, shown in Figure 1, we varied the transceiver bandwidth up to 70 GHz and the VNLE NL memory from 0 to 20 samples. We started by showing the impact of the normalized peak-to-peak amplitude of the in-phase signal $V_{PP,I}/V_\pi$ by optimizing $V_{PP,I}$ for options VNLE and SQRT + VNLE. Figures 2–5 shows the system performance when $L = 20$ km and $TOP = 15$ dBm, in terms of the maximum ODN loss as a function of TX

and RX bandwidth and of the normalized amplitude $V_{PP,I}/V_\pi$, for *NL memory* = 5 samples, 10 samples, 15 samples and 20 samples, respectively. Note that the pre-compensated length L_C is optimized for each pair of the two parameters. The optimum L_C is slightly smaller than the fiber length L , and the difference ΔL between L and L_C increases with TOP. For instance, L_C is around 18 km when L = 20 km and TOP = 15 dBm. This phenomenon is due to the interaction between the fiber Kerr effect and the chromatic dispersion, as explained in [15,31].

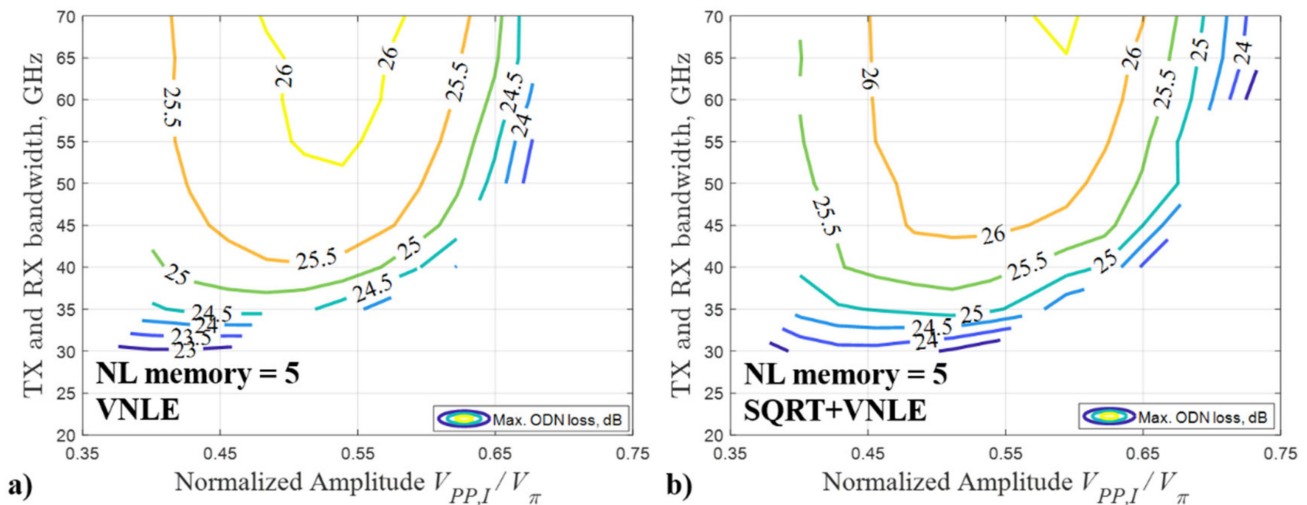


Figure 2. Maximum ODN loss at $BER_T = 10^{-2}$ as a function of TX and RX bandwidth and of the normalized peak-to-peak amplitude of the in-phase signal $V_{PP,I}/V_\pi$ with *NL memory* = 5 samples. The fiber length is L = 20 km. The transmitted optical power is TOP = 15 dBm: (a) VNLE; and (b) SQRT + VNLE.

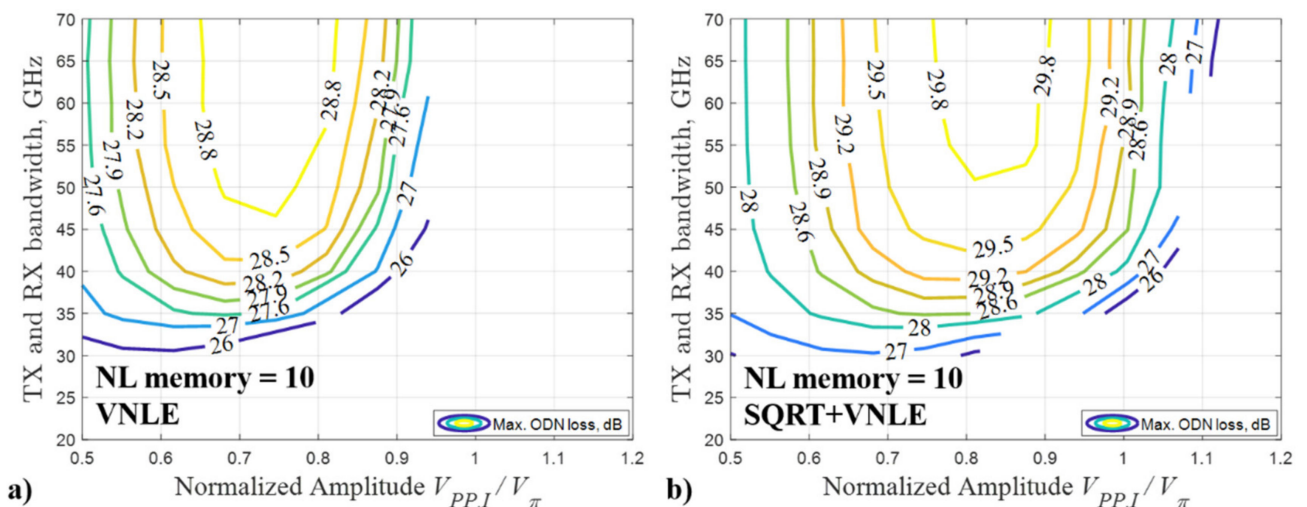


Figure 3. Maximum ODN loss at $BER_T = 10^{-2}$ as a function of TX and RX bandwidth and of the normalized peak-to-peak amplitude of the in-phase signal $V_{PP,I}/V_\pi$ with *NL memory* = 10 samples. The fiber length is L = 20 km. The transmitted optical power is TOP = 15 dBm: (a) VNLE; and (b) SQRT + VNLE.

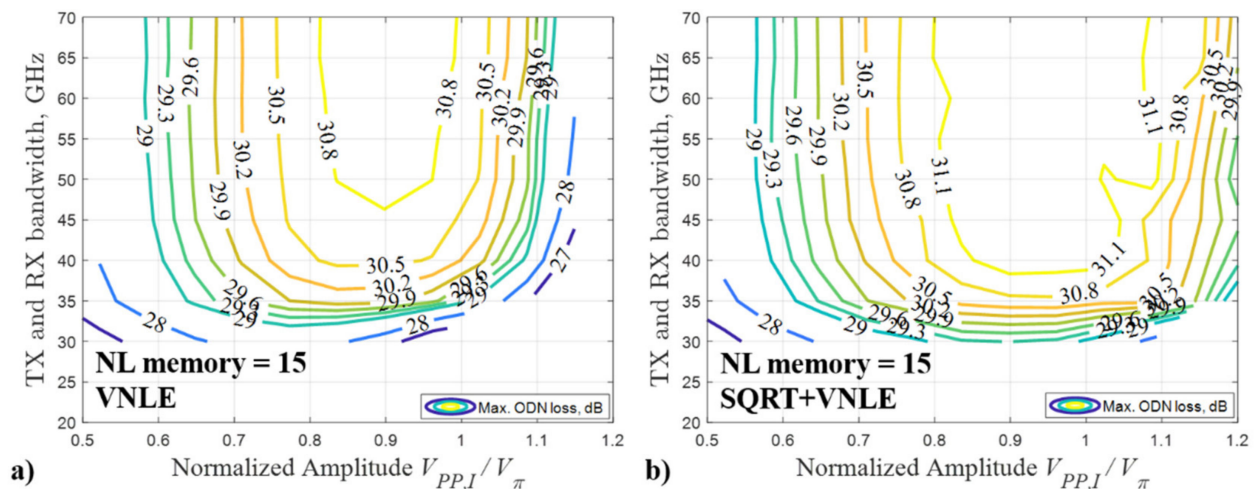


Figure 4. Maximum ODN loss at $BER_T = 10^{-2}$ as a function of TX and RX bandwidth and of the normalized peak-to-peak amplitude of the in-phase signal $V_{PP,I}/V_\pi$ with $NL\ memory = 15$ samples. The fiber length is $L = 20$ km. The transmitted optical power is $TOP = 15$ dBm: (a) VNLE; and (b) SQRT + VNLE.

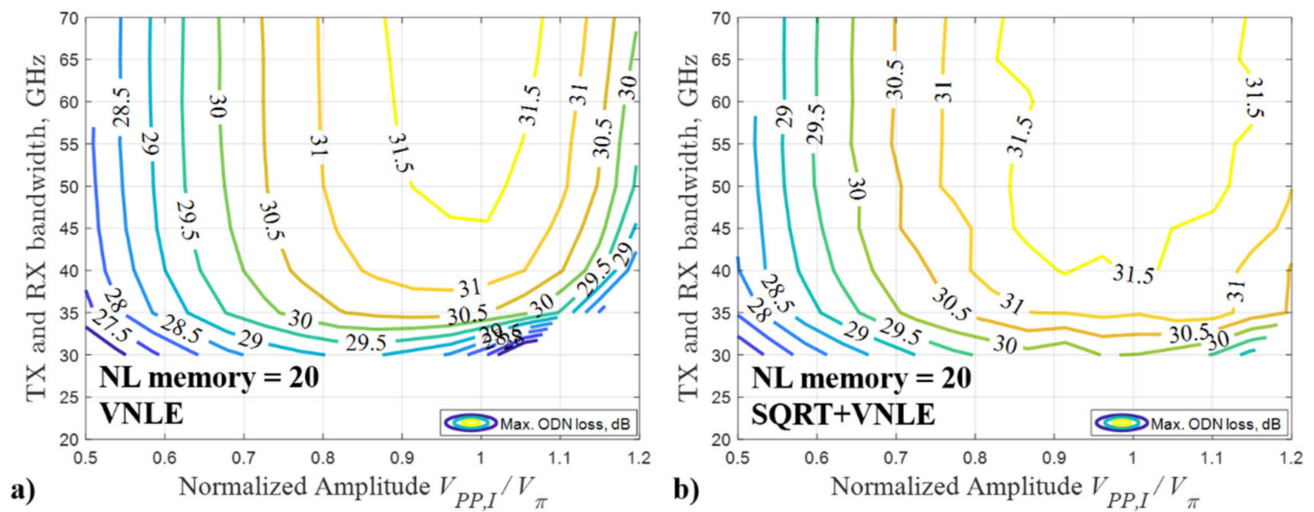


Figure 5. Maximum ODN loss at $BER_T = 10^{-2}$ as a function of TX and RX bandwidth and of the normalized peak-to-peak amplitude of the in-phase signal $V_{PP,I}/V_\pi$ with $NL\ memory = 20$ samples. The fiber length is $L = 20$ km. The transmitted optical power is $TOP = 15$ dBm: (a) VNLE; and (b) SQRT + VNLE.

From Figures 2–5, we can observe that the optimum normalized amplitude $V_{PP,I}/V_\pi$ is in the range 0.55–0.60, 0.70–0.90, 0.90–1.00 and 1.00–1.10 for the VNLE NL memory equal to 5 samples, 10 samples, 15 samples and 20 samples, respectively. The optimum normalized amplitude $V_{PP,I}/V_\pi$ increases as the NL memory increases. This can be explained considering the effect of the optical modulation index (OMI) on the nonlinearities generated in the modulation process. The OMI can be used to find the optimum operation point (at which the highest modulation levels can be obtained without introducing additional distortions) [32]. Smaller $V_{PP,I}/V_\pi$ results in lower nonlinearity of the modulation, but also into a lower modulation level. In contrast, larger $V_{PP,I}/V_\pi$ can result in a higher modulation level but also in stronger nonlinear effects of the modulation. Therefore, it is very important to set the optimum driving signal amplitude by optimizing the normalized amplitude $V_{PP,I}/V_\pi$. Without TX and RX bandwidth limitations and at the optimum $V_{PP,I}/V_\pi$, when the VNLE is applied alone, the maximum ODN loss of about 26.1 dBm,

29.1 dBm, 31.0 dBm, and 31.7 dBm can be reached for $NL\ memory = 5$ samples, 10 samples, 15 samples and 20 samples, respectively; when SQRT + VNLE is applied, the maximum ODN loss of about 26.6 dBm, 30.0 dBm, 31.7 dBm, and 32.0 dBm can be reached for $NL\ memory = 5$ samples, 10 samples, 15 samples and 20 samples, respectively. The VNLE can provide up to 3 dB improvement for every five samples additional NL memory, while the SQRT can provide about 0.5–1.0 dB improvement compared to the VNLE only option. However, the complexity of the VNLE is much higher than that of the SQRT (the complexity will be discussed and analyzed in detail in the following section). It is a trade-off between the system performance and the complexity of RX DSP options.

In addition to the modulation nonlinear effect and the fiber Kerr nonlinear effect, the nonlinear effect in the electrical domain caused by chromatic dispersion after the modulus square operation of DD (DD is inherently nonlinear due to the square-law detection) can be mitigated by using the SQRT as shown in [30]. By comparing Figures 2–5, we can also notice that the optimum normalized amplitude $V_{PP,I}/V_\pi$ of the option SQRT + VNLE is slightly larger than that of the VNLE method (with the same NL memory). Therefore, a higher OMI can be set using VNLE with high NL memory combined with the SQRT, which allows to compensate for stronger nonlinear distortion.

Figure 6 shows the maximum ODN loss as a function of TX and RX bandwidth and of the VNLE NL memory at the optimum normalized amplitude $V_{PP,I}/V_\pi$, for 20 km SMF. On the x-axis, the VNLE $NL\ memory$ equal to 0 corresponds to the SQRT + FFE + DFE technique used in the receiver DSP. This option, which does not include the VNLE, is used as the lowest complexity reference case. Note that, in all cases, the transmitted optical power, the normalized amplitude $V_{PP,I}/V_\pi$ and the pre-compensated length L_C are optimized. The optimum TOP is 11 dBm and 15 dBm for the SQRT + FFE + DFE and VNLE techniques, respectively. We limit our analysis to TOP = 15 dBm as higher transmitted power levels are unrealistic in PON applications. The optimum L_C is 19 km for SQRT + FFE + DFE (with 11 dBm TOP) and 18 km for the VNLE (with 15 dBm TOP). The optimum L_C decreases as TOP increases. This is related to the fact that a higher transmitted optical power results in a higher fiber nonlinear interference [33], which partially counteracts CD due to interaction between the CD and the Kerr effect [15,31]. At the very demanding 200 Gbps rate, the system performance is very poor (maximum ODN loss <23 dB) when strong TX and RX bandwidth limitations are present (i.e., ≤ 25 GHz) even when using the most complex DSP approach (VNLE + SQRT with $NL\ memory = 20$ samples). For SQRT + FFE + DFE (i.e., $NL\ memory = 0$), the largest maximum ODN loss is only about 25 dB even if using very high 70 GHz TX and RX bandwidth. Therefore, this simple DSP solution is not enough to meet the ODN loss requirement with PAM-8 200 Gbps transmission. By using the VNLE, both alone and in combination with the SQRT, a considerable gain can be obtained when we increase the NL memory. As shown in Figures 2–6, about 3 dB, 5 dB and 6 dB maximum ODN loss increase can be obtained when the NL memory is increased from 5 samples to 10 samples, 15 samples and 20 samples, respectively. The trend shows that the improvement would be very limited by further increasing the NL memory above 20 samples. This means that almost all the fiber nonlinear interference is compensated for by the VNLE. About a 3 dB gain in terms of maximum ODN loss can be obtained by relaxing the TX and RX bandwidth limitation from 30 GHz to 50 GHz, with the same NL memory. As shown in Figure 6, for a fixed NL memory value, the improvement is more evident when increasing the TX and RX bandwidth from 30 to 40 GHz. When the TX and RX bandwidth are above 50 GHz, only very limited improvement can be obtained when TX and RX bandwidth are increased.

System performance cannot be usually enhanced by relaxing the bandwidth limitations. More powerful RX DSP options are needed. Comparing the VNLE and the SQRT + VNLE, we observe a non-negligible ODN loss gain of about 1 dB, at the cost of slightly increased complexity due to the SQRT. Moreover, in some cases the overall complexity can be reduced by introducing the SQRT. As shown in Figure 6a), in the 35 GHz to 40 GHz TX and RX bandwidth range representing commercially available 50G-O/E [23],

the VNLE approach requires NL memory from 12 samples to 13 samples to achieve 29 dB maximum ODN loss, whereas a lower 9 samples to 11 samples NL memory is needed when combining the VNLE and the SQRT (see Figure 6b)). This reduction in NL memory can provide a significant improvement in RX DSP complexity in terms of MPS, which will be discussed later. When $NL\ memory = 20$ samples is applied, the 29 dB maximum ODN loss can be reached even with 30 GHz TX and RX bandwidth, at the cost of a very high DSP complexity (which will be discussed later).

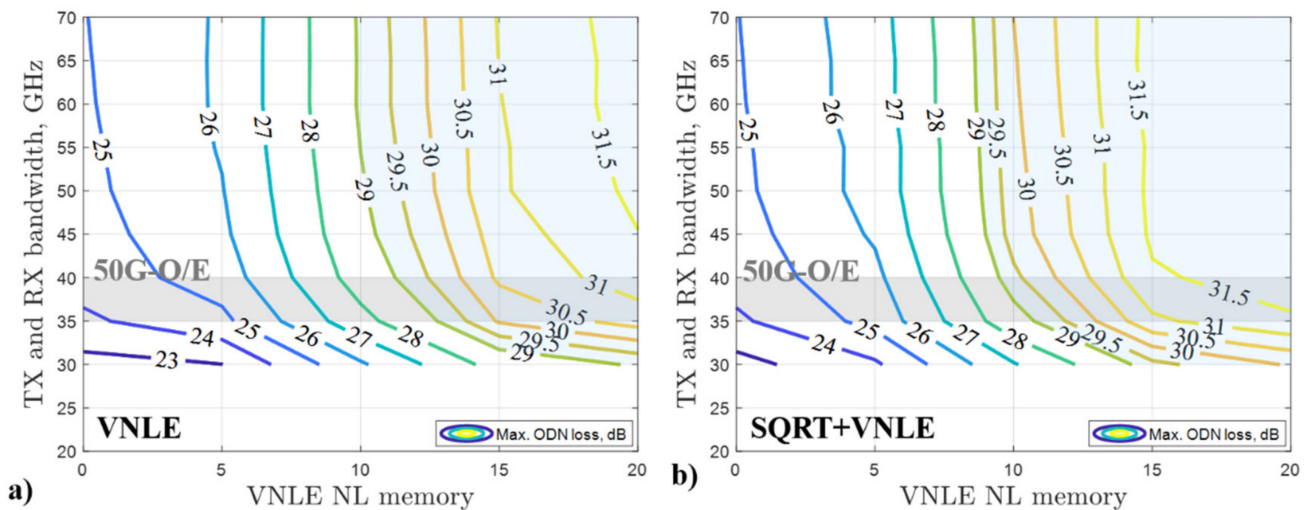


Figure 6. Maximum ODN loss at $BER_T = 10^{-2}$ as a function of TX/RX bandwidth and nonlinear memory of VLNE. The fiber length is $L = 20$ km: (a) VNLE; and (b) SQRT + VNLE. The light blue area is where ODN loss is above 29 dB, and the light grey area is where commercial 50G-O/E are considered. The VNLE NL memory = 0 is equivalent to RX DSP option SQRT + FFE + DFE. TOP is 11 dBm for SQRT + FFE + DFE and 15 dBm for all other RX DSP options.

It is typical in PON architectures that each served ONU is located at a different distance from the OLT. In Figure 7, we present the maximum ODN loss as a function of fiber link lengths L ranging from 5 km to 20 km, which is the typical reach range in PONs. TX and RX bandwidth is set to 37.5 GHz, a typical value for 50G-O/E devices [23]. In all cases, the normalized amplitude $V_{PP,I}/V_{\pi}$ and the pre-compensated length L_C are optimized. For $L = 5$ km, the optimum L_C is 4 km and 4.5 km for the VNLE and the SQRT + VNLE, respectively. The optimum L_C is 9 km, 14 km, and 18 km for L equal to 10 km, 15 km, and 20 km, respectively. We select the VNLE $NL\ memory = 5$ samples, 10 samples and 20 samples. The maximum ODN loss gain obtained by increasing the NL memory increases as the fiber length L increases. At very short distance, for example $L = 5$ km, the improvement is negligible due to the limited nonlinear distortions introduced by the fiber. To achieve 29 dB ODN loss, only $NL\ memory = 5$ samples is required for $L \leq 14$ km, whereas $NL\ memory = 10$ samples is required for L in the 15–20 km range.

In PON solutions, the ONU is the most cost-sensitive element. Here we compare the complexity in terms of MPS of different RX DSP options, which are placed at the ONU side in the downstream transmission. The MPS of the SQRT, FFE, and DFE techniques can be calculated as described in [17]. For the VNLE, the MPS can be evaluated by using Equation (5) in [34]. In this paper, the order of VNLE is equal to 3, the linear memory is 121 samples, and the quadratic and cubic memory (NL memory) are equal to 5 samples, 10 samples, 15 samples or 20 samples. The complexity in terms of MPS of the different RX DSP used in the paper is summarized in Table 1. The least complex method that allows us to achieve 29 dB maximum ODN loss with 50G-O/E devices (indicated with an asterisk in Table 1) is the SQRT + VNLE with $NL\ memory = 10$ samples, requiring 893 MPS. Small

increments in NL memory (especially in cubic memory) can introduce a significant increase in complexity.

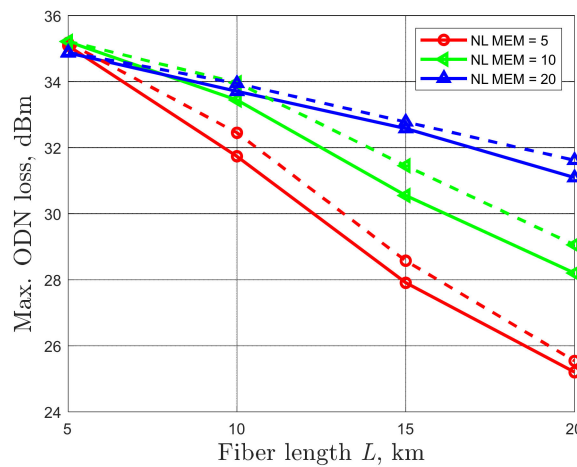


Figure 7. Maximum ODN loss as a function of fiber length targeting $BER_T = 10^{-2}$, for 50G-O/E devices. The normalized amplitude $V_{PP,I}/V_{\pi}$ and the pre-compensated length L_C are optimized for each case. The transmitted optical power $TOP = 15$ dBm. Solid: VNLE, Dashed: SQRT + VNLE.

Table 1. Complexity comparison in terms of multiplication per sample (MPS) for different RX DSP options.

RX DSP Options	NL Memory of VNLE	MPS
SQRT ¹ + FFE ² + DFE ³	-	127
VNLE ⁴	5	256
	10	891
	15	2401 *
	20	5161 *
SQRT ¹ + VNLE ⁴	5	258
	10	893 *
	15	2403 *
	20	5163 *

¹ SQRT requires two additional MPS. It is implemented by using the second order polynomial function as shown in [16]. ² For FFE, MPS equals the number of FFE taps N_{FFE} . ³ For DFE, MPS equals the number of DFE taps N_{DFE} . Note: DFE requires additional implementation MPS due to the feedback loop. ⁴ The MPS of VNLE is evaluated by using the method in [34]. * 29 dB maximum ODN loss can be achieved with 50G-O/E devices.

Although VNLE is an effective RX DSP option to compensate for linear and non-linear distortion, its complexity can be extremely high. The SQRT provides a marginal performance improvement but at the cost of a limited complexity enhancement by only 2 MPS. Thus, the SQRT can be used in combination with the VNLE to decrease the NL memory as well as maintain the desired system performance. For example, as shown in Figure 6, to achieve ≥ 29 dB maximum ODN loss by using 50G O/E, when the VNLE is applied alone, NL memory of 12 samples and 13 samples is required for TX and RX bandwidth of 40 GHz and 35 GHz, respectively, which corresponds to MPS of 1369 and 1668. For the SQRT + VNLE technique, NL memory of 9 samples and 11 samples is needed for TX and RX bandwidth of 40 GHz and 35 GHz, respectively, which corresponds to MPS of 706 and 1111, respectively.

4. Discussion and Conclusions

We demonstrated through simulations the feasibility of 200 Gbps per λ PAM-8 downstream PON transmission in C-band over up to 20 km SMF, preserving DD scheme, achieving 29 dB maximum ODN loss with different RX DSP options. We analyzed the impact

of the peak-to-peak amplitude of the signals, which must be optimized to obtain the best system performance. The VNLE and the SQRT can partially compensate for the nonlinear distortions, and allow a higher optimum normalized amplitude $V_{PP,I}/V_\pi$, resulting in a higher OMI and better system performance. Using the SQRT + FFE + DFE method, without VNLE, 29 dB maximum ODN loss cannot be reached even considering a very large 70 GHz TX and RX bandwidth. For 20 km transmission with 50G O/E devices, when the NL memory of the VNLE is higher than 12 samples, 29 dB maximum ODN loss can be reached by using the VLNE alone. The minimum required NL memory is reduced to 9 samples when the SQRT is combined with the VNLE. Although the reduction in terms of NL memory is relatively small, the resulting reduction in RX DSP complexity (evaluated in terms of MPS) is remarkable. The SQRT + VNLE requires 706 MPS, whereas 1369 MPS are needed for the VNLE alone. This confirms that the SQRT can be used in combination with VNLE to decrease the NL memory (and eventually the RX DSP complexity) while preserving the required link loss budget. We also studied the impact of different RX DSP options for different fiber length. Our findings show that, 200 Gbps PAM-8 communication can be achieved with 29 dB maximum ODN loss by using a variable number of NL memory equal to 5 samples and 10 samples in the 5–14 km and 15–20 km link length ranges, respectively.

Author Contributions: Conceptualization, R.G., V.F., R.M., G.R., P.T.-F. and H.W.; methodology, R.G., V.F., R.M., G.R., P.T.-F. and H.W.; software, P.T.-F. and H.W.; validation, R.G., V.F., R.M., G.R., P.T.-F. and H.W.; formal analysis, R.G., V.F., R.M., G.R., P.T.-F. and H.W.; investigation, R.G., V.F., R.M., G.R., P.T.-F. and H.W.; resources, R.G., V.F., R.M., G.R., P.T.-F. and H.W.; data curation, H.W.; writing—original draft preparation, H.W.; writing—review and editing, R.G., V.F., R.M., G.R., P.T.-F. and H.W.; visualization, R.G., V.F., R.M., G.R., P.T.-F. and H.W.; supervision, R.G., R.M. and V.F.; project administration, R.G., R.M. and V.F. All authors have read and agreed to the published version of the manuscript.

Funding: This research received no external funding.

Institutional Review Board Statement: Not applicable.

Informed Consent Statement: Not applicable.

Data Availability Statement: Not applicable.

Acknowledgments: We thank the support of the PhotoNext initiative at Politecnico di Torino. This work was carried out in the framework of a research contract with Telecom Italia Lab (the TIM company research laboratory).

Conflicts of Interest: The authors declare no conflict of interest.

References

1. Higher Speed Passive Optical Networks, ITU-T G.9804.x Series of Recommendations. G.9804.1 Consented. July 2019. Available online: <https://www.itu.int/rec/T-REC-G.9804.1-201911-I/en> (accessed on 25 February 2022).
2. Wey, J.S. The Outlook for PON Standardization: A Tutorial. *J. Lightwave Technol.* **2020**, *38*, 31–42. [\[CrossRef\]](#)
3. Houtsma, V.; Mahadevan, A.; Kaneda, N.; van Veen, D. Transceiver technologies for passive optical networks: Past, present, and future [Invited Tutorial]. *J. Opt. Commun. Netw.* **2021**, *13*, A44–A55. [\[CrossRef\]](#)
4. Zhang, D.; Liu, D.; Wu, X.; Nessel, D. Progress of ITU-T higher speed passive optical network (50G-PON) standardization. *J. Opt. Commun. Netw.* **2020**, *12*, D99–D108. [\[CrossRef\]](#)
5. Wey, J.S.; Zhang, J. Passive Optical Networks for 5G Transport: Technology and Standards. *J. Lightwave Technol.* **2019**, *37*, 2830–2837. [\[CrossRef\]](#)
6. Zou, J.; Sasu, S.A.; Lawin, M.; Dochhan, A.; Elbers, J.-P.; Eiselt, M. Advanced optical access technologies for next-generation (5G) mobile networks [Invited]. *J. Opt. Commun. Netw.* **2020**, *12*, D86–D98. [\[CrossRef\]](#)
7. Tomkos, I.; Klonidis, D.; Pikasis, E.; Theodoridis, S. Toward the 6G Network Era: Opportunities and Challenges. *IT Prof.* **2020**, *22*, 34–38. [\[CrossRef\]](#)
8. De Alwis, C.; Kalla, A.; Pham, Q.V.; Kumar, P.; Dev, K.; Hwang, W.J.; Liyanage, M. Survey on 6G Frontiers: Trends, Applications, Requirements, Technologies and Future Research. *IEEE Open J. Commun. Soc.* **2021**, *2*, 836–886. [\[CrossRef\]](#)
9. van Veen, D.; Houtsma, V. Strategies for economical next-generation 50G and 100G passive optical networks [Invited]. *J. Opt. Commun. Netw.* **2020**, *12*, A95–A103. [\[CrossRef\]](#)

10. Zhang, J.; Yu, J.; Wey, J.S.; Li, X.; Zhao, L.; Wang, K.; Kong, M.; Zhou, W.; Xiao, J.; Xin, X.; et al. SOA Pre-Amplified 100 Gb/s/λ PAM-4 TDM-PON Downstream Transmission Using 10 Gbps O-Band Transmitters. *J. Lightwave Technol.* **2020**, *38*, 185–193. [\[CrossRef\]](#)

11. Saber, M.G.; Gutiérrez-Castrejón, R.; Alam, M.S.; Xing, Z.; El-Fiky, E.; Xu, L.; Cavaliere, F.; Vall-Llosera, G.; Lessard, S.; Plant, D.V. 100 Gb/s/λ Duo-Binary PAM-4 Transmission Using 25G Components Achieving 50 km Reach. *IEEE Photonics Technol. Lett.* **2020**, *32*, 138–141. [\[CrossRef\]](#)

12. Erkilinc, M.S.; Emmerich, R.; Habel, K.; Jungnickel, V.; Schmidt-Langhorst, C.; Schubert, C.; Freund, R. PON transceiver technologies for ≥ 50 Gbits/s per λ : Alamouti coding and heterodyne detection. *J. Opt. Commun. Netw.* **2020**, *12*, A162–A170. [\[CrossRef\]](#)

13. Che, D.; Iannone, P.; Raybon, G.; Matsui, Y. 200 Gb/s Bi-Directional TDM-PON with 29-dB Power Budget. In Proceedings of the 2021 European Conference on Optical Communication (ECOC), Bordeaux, France, 13–16 September 2021; pp. 1–3. [\[CrossRef\]](#)

14. Torres-Ferrera, P.; Wang, H.; Ferrero, V.; Gaudino, R. 100 Gbps/λ PON downstream O- and C-band alternatives using direct-detection and linear-impairment equalization. *J. Opt. Commun. Netw.* **2021**, *13*, A111–A123. [\[CrossRef\]](#)

15. Torres-Ferrera, P.; Rizzelli, G.; Ferrero, V.; Gaudino, R. 100+ Gbps/λ 50 km C-Band Downstream PON Using CD Digital Pre-Compensation and Direct-Detection ONU Receiver. *J. Lightwave Technol.* **2020**, *38*, 6807–6816. [\[CrossRef\]](#)

16. Wang, H.; Torres-Ferrera, P.; Rizzelli, G.; Ferrero, V.; Gaudino, R. 100 Gbps/λ C-Band CD Digital Pre-Compensated and Direct-Detection Links with Simple Non-Linear Compensation. *IEEE Photonics J.* **2021**, *13*, 7200908. [\[CrossRef\]](#)

17. Torres-Ferrera, P.; Rizzelli, G.; Wang, H.; Ferrero, V.; Gaudino, R. Experimental Demonstration of 100 Gbps/λ C-Band Direct-Detection Downstream PON Using Non-Linear and CD Compensation with 29 dB+ OPL Over 0 Km–100 Km. *J. Lightwave Technol.* **2020**, *40*, 547–556. [\[CrossRef\]](#)

18. Zhu, Y.; Yi, L.; Yang, B.; Huang, X.; Wey, J.S.; Ma, Z.; Hu, W. Comparative study of cost-effective coherent and direct detection schemes for 100 Gb/s/λ PON. *J. Opt. Commun. Netw.* **2020**, *12*, D36–D47. [\[CrossRef\]](#)

19. Suzuki, N.; Miura, H.; Matsuda, K.; Matsumoto, R.; Motoshima, K. 100 Gb/s to 1 Tb/s Based Coherent Passive Optical Network Technology. *J. Lightwave Technol.* **2018**, *36*, 1485–1491. [\[CrossRef\]](#)

20. Zhang, J.; Jia, Z.; Xu, M.; Zhang, H.; Campos, L.A. Efficient preamble design and digital signal processing in upstream burst-mode detection of 100G TDM coherent-PON. *J. Opt. Commun. Netw.* **2021**, *13*, A135–A143. [\[CrossRef\]](#)

21. Zhang, Z.; Guo, Q.; Ju, C.; Cai, S.; Wang, L.; Zhang, M.; Chen, X. Optical- and Electrical-Domain Compensation Techniques for Next-Generation Passive Optical Networks. *IEEE Commun. Mag.* **2019**, *57*, 144–150. [\[CrossRef\]](#)

22. IEEE Std 802.3ca-2020; IEEE Standard for Ethernet Amendment 9: Physical Layer Specifications and Management Parameters for 25 Gb/s and 50 Gb/s Passive Optical Networks. IEEE: Piscataway, NJ, USA, 2020; pp. 1–267.

23. Harstead, E.; Bonk, R.; Walklin, S.; van Veen, D.; Houtsma, V.; Kaneda, N.; Mahadevan, A.; Borkowski, R. From 25 Gb/s to 50 Gb/s TDM PON: Transceiver architectures, their performance, standardization aspects, and cost modeling. *J. Opt. Commun. Netw.* **2020**, *12*, D17–D26. [\[CrossRef\]](#)

24. Wey, J.S.; Nesson, D.; Valvo, M.; Grobe, K.; Roberts, H.; Luo, Y.; Smith, J. Physical layer aspects of NG-PON2 standards—Part 1: Optical link design. *J. Opt. Commun. Netw.* **2016**, *8*, 33–42. [\[CrossRef\]](#)

25. Rosales, R.; Cano, I.; Nesson, D.; Brenot, R.; Dubrovina, N.; Durán-Valdeiglesias, E.; Debregeas, H. Achieving high budget classes in the downstream link of 50G-PON. *J. Opt. Commun. Netw.* **2021**, *13*, D13–D21. [\[CrossRef\]](#)

26. Spiekman, L.; Piehler, D.; Iannone, P.; Reichmann, K.; Lee, H. Semiconductor Optical Amplifiers for FTTx. In Proceedings of the 2007 9th International Conference on Transparent Optical Networks, Rome, Italy, 1–5 July 2007; pp. 48–50. [\[CrossRef\]](#)

27. Rosales, R.; Cano, I.N.; Nesson, D.; Brenot, R.; Talli, G. 50G-PON Downstream Link up to 40 km with a 1342 nm Integrated EML + SOA. *IEEE Photonics Technol. Lett.* **2022**, *34*, 306–308. [\[CrossRef\]](#)

28. Characteristics of a Single-Mode Optical Fiber and Cable. ITU-T Recommendation G.652. 2009. Available online: <https://www.itu.int/itu-t/recommendations/rec.aspx?rec=13076> (accessed on 25 February 2022).

29. Fritzsch, D.; Lischka, L.; Breuer, D.; Schäffer, C.G. Volterra based nonlinear equalizer with reduced complexity. *Asia-Pac. Opt. Commun.* **2007**, *6783*, 448–455. [\[CrossRef\]](#)

30. Prat, J.; Napoli, A.; Gene, J.M.; Omella, M.; Poggiglioli, P.; Curri, V. Square root strategy: A novel method to linearize an optical communication system with electronic equalizers. In Proceedings of the 2005 31st European Conference on Optical Communication, Glasgow, UK, 25–29 September 2005; Volume 3, pp. 713–714. [\[CrossRef\]](#)

31. Poggiglioli, P.; Bosco, G.; Carena, A.; Curri, V.; Jiang, Y.; Forghieri, F. The GN-Model of Fiber Non-Linear Propagation and its Applications. *J. Lightwave Technol.* **2014**, *32*, 694–721. [\[CrossRef\]](#)

32. M2 Optics, Inc. Defining Optical Modulation Index. Available online: https://www.globalspec.com/m2optics/ref/Defining_OMI.pdf (accessed on 5 January 2022).

33. Chen, Z.; Yan, L.; Pan, W.; Luo, B.; Zou, X.; Jiang, H. A Transmission Model of Analog Signals in Photonic Links. *IEEE Photonics J.* **2014**, *6*, 7903813. [\[CrossRef\]](#)

34. Tsimbinos, J.; Lever, K.V. The computational complexity of nonlinear compensators based on the Volterra inverse. In Proceedings of the 8th Workshop on Statistical Signal and Array Processing, Corfu, Greece, 24–26 June 1996; pp. 387–390. [\[CrossRef\]](#)